DOI: 10.1007/s11099-017-0708-1 PHOTOSYNTHETICA 56 (2): 567-577, 2018

Response of photosystem II performance and antioxidant enzyme activities in stay-green wheat to cytokinin

D.Q. YANG[#], Y.L. LUO[#], W.H. DONG, Y.P. YIN, Y. LI[+], and Z.L. WANG[+]

State Key Laboratory of Crop Biology, Shandong Agricultural University, Tai'an – 271018, Shandong, China

Abstract

WN6 (a stay-green wheat cultivar) and JM20 (control) were used to evaluate the effects of exogenous cytokinin on photosynthetic capacity and antioxidant enzymes activities in flag leaves. Results showed that WN6 reached the higher grain mass, which was mainly due to the higher photosynthetic rate resulting from the higher maximal quantum yield of PSII photochemistry (Φ_{PSII}) and probability that a trapped exaction transfers an electron into the electron transport chain beyond Q_A (Ψ_o), and lower relative variable fluorescence intensity at the J-step (V_j). Exogenous 6-benzylaminopurine (6-BA) enhanced antioxidant enzymes activities and decreased malondialdehyde (MDA) content. Enhanced Ψ_o and electron transport rate (ETR), and decreased V_j contributed to improved photosynthetic rate in the 6-BA treatment. In addition, exogenous 6-BA significantly increased endogenous zeatin (Zt) content, which was significantly and positively correlated with the antioxidant enzyme activity and Φ_{PSII}, implying that higher Zt content was responsible for the improved antioxidant status and photosynthetic performance.

Additional key words: chlorophyll fluorescence; gas exchange; growth hormone; JIP test; performance index; peroxidase.

Introduction

Wheat is one of the most important food crops worldwide. Increasing its production contributes to improvement of global food security (Shiferaw *et al*. 2013). Photosynthesis is a major trait available for further increases in a yield potential (Long *et al*. 2006). Increasing evidence has demonstrated that increasing crop photosynthesis could be an important way to meet the challenge of doubling the food production (Zhu *et al*. 2010). Stay-green (SG) wheat cultivars appeared to be associated with a longer functioning leaf area and higher photosynthetic capacity, thereby increasing productivity (Hörtensteiner 2009). However, photosynthetic capacity and green leaf area decline gradually from anthesis and then sharply with leaf aging process (Rajcan and Tollenaar 1999). During this process, leaf cells undergo orderly changes in cell structure, metabolism, and gene expression (Pfannschmidt 2003, Lim *et al*. 2007), which are characterized by events related to increase in reactive oxygen species (ROS), lipid peroxidation, and dismantling of photosynthetic apparatus (Navabpour *et al.* 2003, Pružinská *et al.* 2005, Nishiyama *et al*. 2006). ROS, such as superoxide, singlet oxygen, hydroxyl radical, and hydrogen peroxide are generated at the reaction centers of PSII in chloroplast thylakoids during leaf senescence (Pospíšil 2012). Results inferred

Received 22 May 2016, *accepted* 13 December 2016, *published as online-first* 10 March 2018.
[+]Corresponding authors; e-mail: woooowo@126.com; zlwang@sdau.edu.cn.
Abbreviations: APX – ascorbate peroxidase; CAT – catalase; Chl – chlorophyll; CK – cytokinin; DAA – days after anthesis; ETR – electron transport rate; F_i – the fluorescence at 30 ms; F_j – the fluorescence at 2 ms; F_k – the fluorescence at 300 μs; F_0 – the fluorescence fluorescence at 20 μs; F_m – maximal fluorescence yield of the dark-adapted state; F_m' – maximal fluorescence yield of the light-adapted state; F_s – steady-state fluorescence yield; F_t – fluorescence intensity at t time; F_v – variable fluorescence; F_v/F_m – maximal quantum yield of PSII photochemistry; FM – fresh mass; g_s – stomatal conductance; MDA – malondialdehyde; NSG – non-stay-green; PI_{abs} – performance index based on absorption of light energy; P_N – net photosynthetic rate; POD – peroxidase; ROS – reactive oxygen species; SG – stay-green cultivar; SOD – superoxide dismutase; V_j – relative variable fluorescence intensity at the J-step; W_k – relative variable fluorescence for the normalization between F_o and F_k; Zt – zeatin; Φ_{PSII} – effective quantum yield of PSII photochemistry; Ψ_o – probability that a trapped exaction transfers an electron into the electron transport chain beyond Q_A.
Acknowledgments: The research was supported by the National Natural Science Foundation of China (NO. 31271661, 31271667, 30871477), the Shandong Modern Agriculture Technology and Industry System, a project of Shandong Province Higher Educational Science and Technology Program（J14LF12), the National Basic Research Program of China (973 Program, NO. 2015CB150404), the Special Fund for Agro-scientific Research in the Public Interest of China (No. 201203100, 201203029), and the National Science and Technology Support Program of China (No. 2012BAD04B05).
[#]These authors contributed equally to this study.

that PSII was the vulnerable part of photosynthetic apparatus and easily damaged by superoxide and hydrogen peroxide (Maxwell and Johnson 2000, Tjus *et al*. 2001). Plant cells have evolved sophisticated strategies to keep the concentrations of ROS under control and protect photosynthetic apparatus from oxidative stress (Mittler 2002). One of the protective mechanisms is enzymatic ROS-scavenging system, which includes superoxide dismutase (SOD), peroxidase (POD), catalase (CAT), and ascorbate peroxidase (APX) (Apel and Hirt 2004).

It is widely recognized that antioxidant enzyme activities can be regulated by plant growth regulators. Cytokinins are a class of plant-specific hormones that play a central role during the cell cycle and influence numerous developmental programs (Klerk *et al*. 2001, Werner *et al*. 2001). Studies of Merewitz *et al*. (2011) suggested that cytokinins promoted protein synthesis and maintained the antioxidant responses. Meanwhile, it is also documented that cytokinins could retain the contents of chlorophyll (Chl) in the photosynthetic apparatus in barley and wheat (Yaronskaya *et al*. 2006, Zavaleta-Mancera *et al*. 2007). In addition, some mutants, such as SG mutants of wheat, are characterized by longer green leaf duration and delayed senescence (Thomas and Howarth 2000). This can be the result of alterations in hormone metabolism and signaling, particularly affecting networks involving cytokinins and ethylene (Khanna-Chopra 2012, Thomas and Ougham 2014). However, there is little information about the effects of cytokinin application on photosynthetic characteristics in different SG cultivars during leaf senescence. Moreover, our understanding of differences between SG and non-stay-green (NSG) varieties in PSII performance, is very limited. Chl *a* fluorescence measurement represents a potentially valuable approach to obtain quantitative and quantitative information on photosynthetic apparatus (Baker and Rosenqvist 2004, Kalaji *et al*. 2016). Given that, it can be used to investigate whether and how exogenous 6-BA is involved in regulating PSII performance during leaf senescence. Thus, we carried out experiments with the SG and NSG wheat cultivars sprayed with exogenous 6-BA and lovastatin (an inhibitor of cytokinin synthesis). We attempted to (*1*) identify differences between the two cultivars in antioxidant enzyme activities, PSII performance, and grain mass; (*2*) elucidate the effects of exogenous 6-BA on the function of PSII and antioxidative enzymes activities, and endogenous content of zeatin in SG wheat.

Materials and methods

Plant material and growth conditions: The field experiments were carried out in 2012–2013 at Tai'an Experimental Station of Shandong Agricultural University, Tai'an, China (36°09'N, 117°09'E; 128 m a.s.l.). The climate in this region is warm and semihumid continental monsoon, with an average annual temperature of 13.7°C and an average annual rainfall of 631.5 mm. Two wheat genotypes, stay-green (SG) WN6 and the control variety JM20 (non-stay-green, NSG) were grown in the experimental plots. The plot size was 9 m^2 (3 m × 3 m) with ten rows (0.25 m between rows). The soil type is sandy loam (pH 7.3). The top 30 cm of the soil contained 18.11 g (organic matter) kg^{-1}, 1.23 g(total N) kg^{-1}, 87.2 mg (available N) kg^{-1}, 17.05 mg(Olsen-P) kg^{-1}, and 112.80 mg (Olsen-K) kg^{-1}. Before planting 120 kg(N) ha^{-1}, 75 kg (P_2O_5) ha^{-1}, and 150 kg(K_2O) ha^{-1} were mixed into the soil, and another 120 kg(N) ha^{-1} was applied at the jointing stage. Seeds were sown on 10 October 2012 with the density of 225 plants m^{-2}. The plants were harvested on 14 June 2013, respectively. Pests, diseases, and weeds were controlled by appropriate chemical applications during a crop cycle.

Experimental design: The experiment was 2 × 3 [two cultivars and three exogenous applications (water, cytokinin, and lovastatin)] in factorial design with six treatments. Each treatment was replicated three times in a randomized complete block design. Date of anthesis (stage 65, Zadoks *et al*. 1974) was determined when anthers shed at least 50% of the spike. Synthetic cytokinin (6-benzyl aminopurine, 6-BA), lovastatin (an inhibitor of cytokinin synthesis, Kobayashi *et al*. 2007) (all from *Sigma*, St Louis, MO, USA), were applied to the two cultivars. The preparation of 6-BA and lovastatin solutions were used modified method described by Hu *et al*. (2012) and Crowell and Salaz (1992), respectively. Either 4.5×10^{-5} M 6-BA, or 2.5×10^{-4} M lovastatin were sprayed at the rate of 100 mL m^{-2} on the whole plants between 1 and 3 d after anthesis (DAA) at 17:00 h. Each treatment included an area of 9 m^2 with three replications. All the solutions contained *Tween-20* at final concentrations of 0.5% (v/v) as a surfactant. The control plants were sprayed with the same volume of deionized water, containing the same concentrations of *Tween-20*.

Tagging and sampling flag leaves: Uniform wheat plants flowering on the same day were tagged in the experiment. Thirty tagged flag leaves from each treatment were sampled at 7-d intervals from anthesis to 35 DAA. Flag leaves were detached, immediately submerged in liquid nitrogen for 0.5 h, and then stored at −40°C until biochemical assays were performed.

Determination of endogenous zeatin in leaves: The extraction and purification of zeatin (Zt) were measured by high performance liquid chromatography (HPLC), which was modified from those previously described methods (Zhao *et al*. 2012). The hormone extracts went through 0.2 μm hydrophobic membranes, and then 10 μL samples was injected into a *Waters* symmetry C18 column

(4.6 mm × 150 mm, 5 μm) using acetonitrile:methanol: 0.6% acetic acid solution (5:50:45, v/v/v) as mobile phase. The flow rate was kept at 0.6 mL min^{-1} and the peaks were detected by a photodiode array absorbance detector (*Waters 2998 Separations Module*, USA) at 254 nm.

Assays of antioxidase enzyme activity, Chl, and MDA content: Flag leaves (0.5 g) were crushed and homogenized with 5 ml of 0.05 mol L^{-1} sodium phosphate buffer (pH = 7.8) at 0°C. The homogenate was centrifuged at 10,000 × *g* for 20 min, and the supernatants were used for enzyme activity assays and MDA content determination.

SOD (EC 1.15.1.1.), POD (EC 1.11.1.7.), CAT (EC 1.11.1.6.), and APX (EC 1.11.1.11.) activities were determined according to Zhao *et al*. (2002) using a spectrophotometer *(UV-1901*, *Beijing Purkinje General Instrument Co. Ltd*., Beijing, China). The activity of SOD was measured in a reaction mixture containing 50 mM phosphate buffer (pH 7.8), 0.1 mM EDTA, 130 mM methionine, 0.75 mM nitroblue tetrazolium (NBT), 20 μM riboflavin, and 50 μl of the extract. One unit of SOD activity was defined as the amount of crude enzyme extract that is required for inhibition the reduction rate of NBT by 50%. POD activity was determined by the rate of guaiacol oxidation by H_2O_2. The reaction mixture contained 25 mM phosphate buffer (pH 7.0), 16 mM guaiacol, and 10 μl of 10% H_2O_2, and 20 μl of the extract in a 3 ml volume. POD activity was measured following the increase of absorbance at 420 nm. One unit of POD activity was defined as U mg^{-1}(protein) min^{-1} using the exctinction coefficient of 25.5 mM^{-1} cm^{-1}. CAT was assayed in a reaction mixture containing 2.0 ml of 50 mM phosphate buffer (pH 7.8), 0.5 ml of 30 mM H_2O_2, and 0.1 ml of the extract. The activity was measured by monitoring the disappearance of H_2O_2 by measuring the decrease in absorbance at 240 nm. One unit of CAT activity was defined as U mg^{-1}(protein) min^{-1} using the exctinction coefficient of 39.4 mM^{-1} cm^{-1}. The activity of APX was measured by monitoring the rate of ascorbate oxidation at 290 nm. APX activity was assayed in a reaction mixture containing 0.3 mM ascorbate, 0.06 mM H_2O_2, 0.1 mM EDTA, and 0.1 ml enzyme extract in 50 mM phosphate buffer (pH 7.0). The extinction coefficient of AsA was 2.8 mM^{-1} cm^{-1}. The activity was expressed as μmol(AsA) mg^{-1}(protein) min^{-1}.

The MDA content was measured according to Zhao *et al*. (2002). The extract (1 ml) and 2 ml of 0.6% thiobarbituric acid were boiled for 20 min and cooled to room temperature. The absorbance of MDA was measured at 600, 532, and 450 nm by a spectrophotometer (*UV-1901*, *Beijing Purkinje General Instrument Co. Ltd*., Beijing, China) after centrifugation at 3,000 × *g* for 15 min. MDA concentrations were calculated by the equation:

MDA [μmol g^{-1}(FM)] = [6.45 × (OD_{532} – OD_{600}) – 0.56 × OD_{450}] × V/W, where OD_{532}, OD_{600}, and OD_{450} are the absorbance at 532, 600, and 450 nm, respectively; V is the volume of extraction, W is the fresh mass of sample.

Leaf Chl was extracted with 95% ethyl alcohol in the dark for 24 h at 4°C. The extracts were analyzed using UV-visible spectrophotometer (*UV-1901*, *Beijing Purkinje General Instrument Co. Ltd*., Beijing, China). Chl *a* and *b* was determined at 663 and 646 nm, respectively. Leaf Chl concentration was calculated according to Zhao *et al*. (2002).

Assays of photosynthetic rate and Chl fluorescence: Tagged flag leaves (10) of each treatment were selected to measure gas-exchange parameters of photosynthesis and Chl fluorescence. Photosynthetic rate (P_N) of flag leaves was measured using infrared gas analyzer *CIRAS-2* (*PP-Systems*, Hitchin, UK) at 7-d intervals from anthesis. During the measuring period (09:00–11:00), the ambient CO_2 concentration, light intensity, and temperature in the field and measuring cuvette were about 360 μmol mol^{-1}, PPFD of 1,200 μmol(photon) m^{-2} s^{-1}, and 23°C, respectively, for all the treatments. The chamber was equipped with a red/blue LED light source. The relative air humidity in the chamber was about 70%.

Leaf Chl fluorescence parameters were measured using a pulse-modulated fluorimeter (*FMS-2*, Hitchin, UK). Leaves were kept for 30 min in a dark before measurements. The minimal fluorescence (F_0) was recorded. Then, maximal fluorescence (F_m) was determined using saturation pulse flash of 4,000 μmol(photon) m^{-2} s^{-1} for 0.8 s. Then, the steady-state value of fluorescence (F_s) was determined under actinic light of 400 μmol(photon) m^{-2} s^{-1} for 10 min. The maximal light-adapted fluorescence (F_m') was measured at saturating pulse of 4,000 μmol(photon) m^{-2} s^{-1} for a second. Maximal quantum yield of PSII (F_v/F_m) and the effective quantum yield (Φ_{PSII}) were calculated with the following formulas (Maxwell and Johnson 2000, Maxwell 2002): $F_v/F_m = (F_m - F_0)/F_m$, $\Phi_{PSII} = (F_m' - F_s)/F_m'$. ETR was calculated as Φ_{PSII} × PFDa × 0.5, where PFDa is absorbed PFD calculated using an integrating sphere and 0.5 is used an estimate of the distribution of light energy between PSI and PSII.

The fast Chl fluorescence induction kinetics curve was measured using a *Handy-PEA* chlorophyll fluorometer (*Hansatech*, UK). Flag leaves after 10, 20, and 30 DAA were dark-adapted for 30 min and then illuminated with continuous red light for 1 s at 3,000 μmol(photon) m^{-2} s^{-1}. The data were available to be treated according to the equations of the JIP test parameters by any tabulation program and were analyzed using the JIP test (Strasser 1997, Strasser *et al*. 2000, Schansker *et al.* 2003). The following parameters were used in this study:

Chl fluorescence parameters	Fluorescence	Phase
F_o	at 20 μs	O
F_k	at 300 μs	K
F_j	at 2 ms	J
F_i	at 30 ms	I
F_m	maximal fluorescence	P
V_k	relative variable fluorescence	K
V_j	relative variable fluorescence	J
V_i	relative variable fluorescence	I
W_k	the normalized relative variable fluorescence	K step

Ψ_o was the probability that a trapped exaction transfers an electron into the electron transport chain beyond Q_A. PI_{abs} was the performance index based on absorption of light energy.

Statistical analysis was carried out using *PASW* software *version 18.0*. The data from each sampling date were analyzed separately and the means were tested by the least significant difference at the $P_{0.05}$ level ($LSD_{0.05}$).

Results

Grain mass: The grain mass of WN6 was higher than that of JM20. Compared with the control treatment, the grain mass significantly increased by exogenous 6-BA application in both cultivars (Fig. 1). Compared with the control, the grain mass in WN6 increased by 5.6%. By contrast, grain mass in JM20 increased by 12.0%. However, application of lovastatin significantly reduced the grain mass.

Chl and MDA contents in flag leaves: The contents of Chl in two cultivars decreased continuously from 7 to 35 DAA, while contents of MDA increased gradually (Fig. 2). The Chl contents in SG wheat WN6 were significantly higher than those in JM20 from 7 to 35 DAA. But MDA contents in flag leaves of WN6 were lower than those in flag leaves of JM20. Exogenous 6-BA significantly increased the Chl contents in the leaves from 7 to 35 DAA. Application of lovastatin significantly decreased Chl contents and increased the MDA contents.

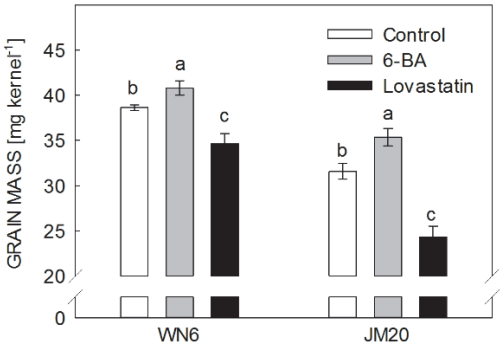

Fig. 1. Effect of 6-BA and lovastatin on grain mass of a stay-green (WN6) and a non-stay-green (JM20) wheat cultivar. *Vertical bars* represent ± SE of the mean (n = 3) where these exceed the size of the symbol. *Different letters* indicate significant differences between treatments at P<0.05.

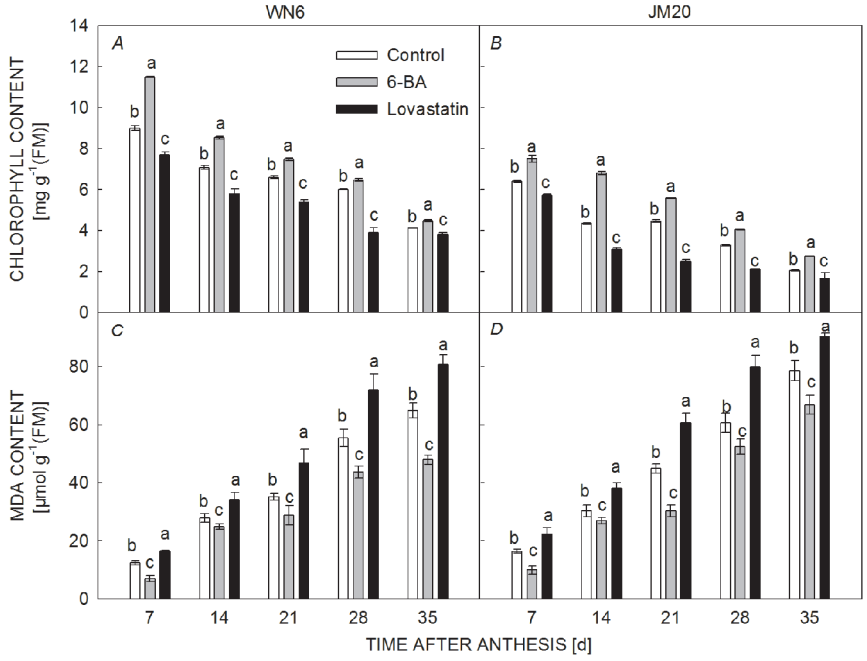

Fig. 2. Effect of 6-BA and lovastatin on chlorophyll (*A,B*) and malondialdehyde (MDA) (*C,D*) contents in leaves of a stay-green (WN6) and a non-stay-green (JM20) wheat cultivar. *Vertical bars* represent ± SE of the mean (n = 3). *Different letters* indicate significant differences between treatments at P<0.05.

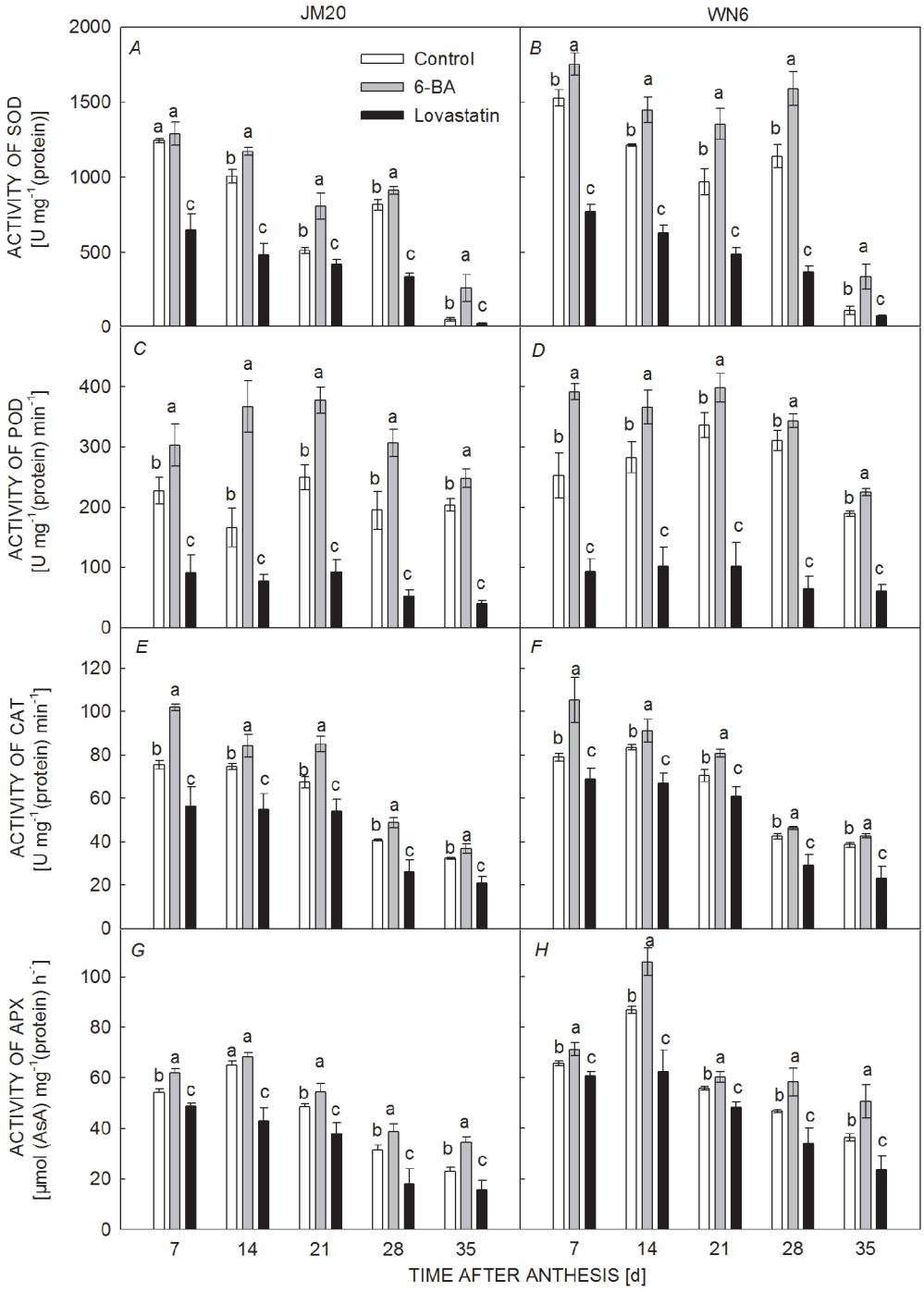

Fig. 3. Effect of 6-BA and lovastatin on superoxide dismutase (SOD) (*A,B*), peroxidase (POD) (*C,D*), catalase (CAT) (*E,F*), and ascorbate peroxidase (APX) (*G,H*) activity in leaves of a stay-green (WN6) and a non-stay-green (JM20) wheat cultivar. *Vertical bars* represent ± SE of the mean (n = 3). *Different letters* indicate significant differences between treatments at P<0.05.

Activities of SOD, POD, CAT, and APX in flag leaves: The activities of SOD and CAT decreased continuously from 7 to 35 DAA, whereas POD and APX activities reached a maximum at 21 and 14 DAA, respectively, and declined thereafter (Fig. 3). These activities were higher in the WN6 than that in JM20 from 7 to 35 DAA. Under the 6-BA treatment, the activities significantly increased when compared with those under the control treatment. Conversely, the application of lovastatin showed an opposite effect. The activities of enzymes significantly decreased by lovastatin treatment from 7 to 35 DAA.

Photosynthesis: The net photosynthetic rate (P_N) and stomatal conductance (g_s) of flag leaves gradually were

lowered from anthesis (Fig. 4*A–D*). The P_N was higher in the flag leaf of WN6 than that in JM20 at 7 to 35 DAA. The two cultivars responded similarly to the 6-BA and lovastatin treatment. Exogenous application of 6-BA significantly increased the P_N and g_s of the flag leaves compared with the controls. In contrast, the P_N and g_s of two cultivars decreased by exogenous lovastatin treatment.

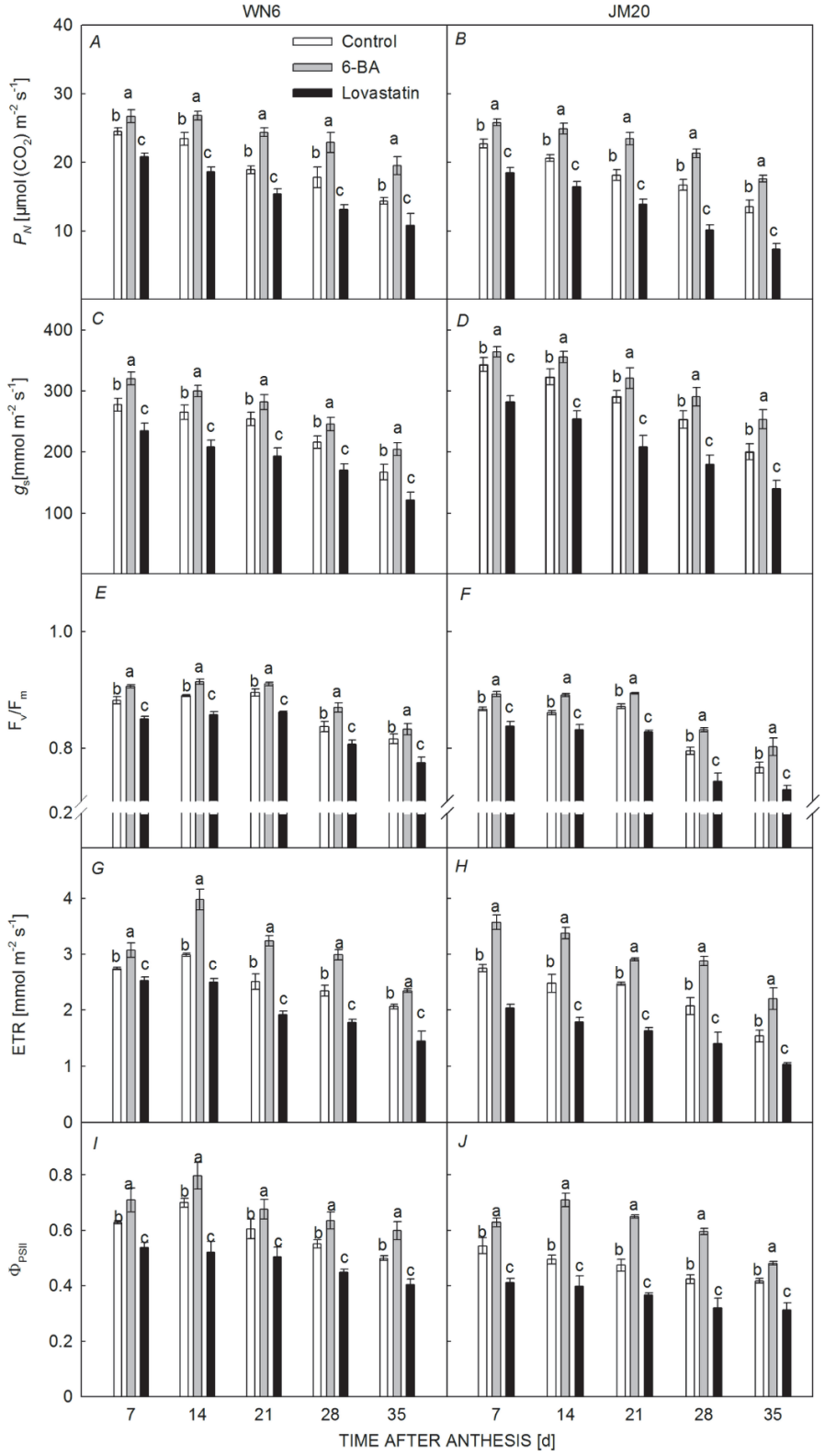

Fig. 4. The effects of 6-BA and lovastatin net photosynthetic rate (P_N) (*A,B*), stomatal conductance (g_s) (*C,D*), maximal quantum yield of PSII photochemistry (F_v/F_m) (*E,F*), electron transport rate (ETR) (*G,H*), effective quantum yield of PSII photochemistry (Φ_{PSII}) (*I,J*) of a stay-green (WN6) and a non-stay-green (JM20) wheat cultivar. *Vertical bars* represent ± SE of the mean (n = 10) where these exceed the size of the symbol. *Different letters* indicate significant differences among each treatment, $P<0.05$.

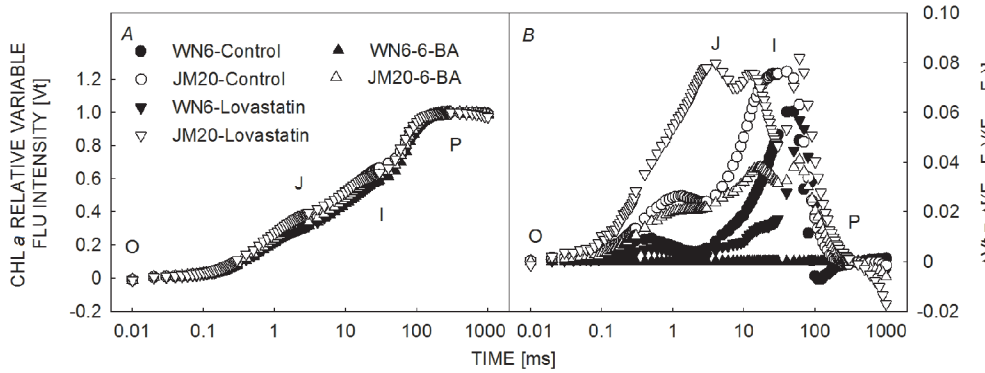

Fig. 5. The effects of 6-BA and lovastatin on the difference between the variable fluorescence induction kinetics curve (Vt, *A*) and the relative fluorescence induction kinetics curve (ΔVt, *B*) of PSII in leaves at 20 DAA. O–O step at about 20 ms; J–J step at about 2 ms; I–I step at about 30 ms; P–P step, the maximum fluorescence.

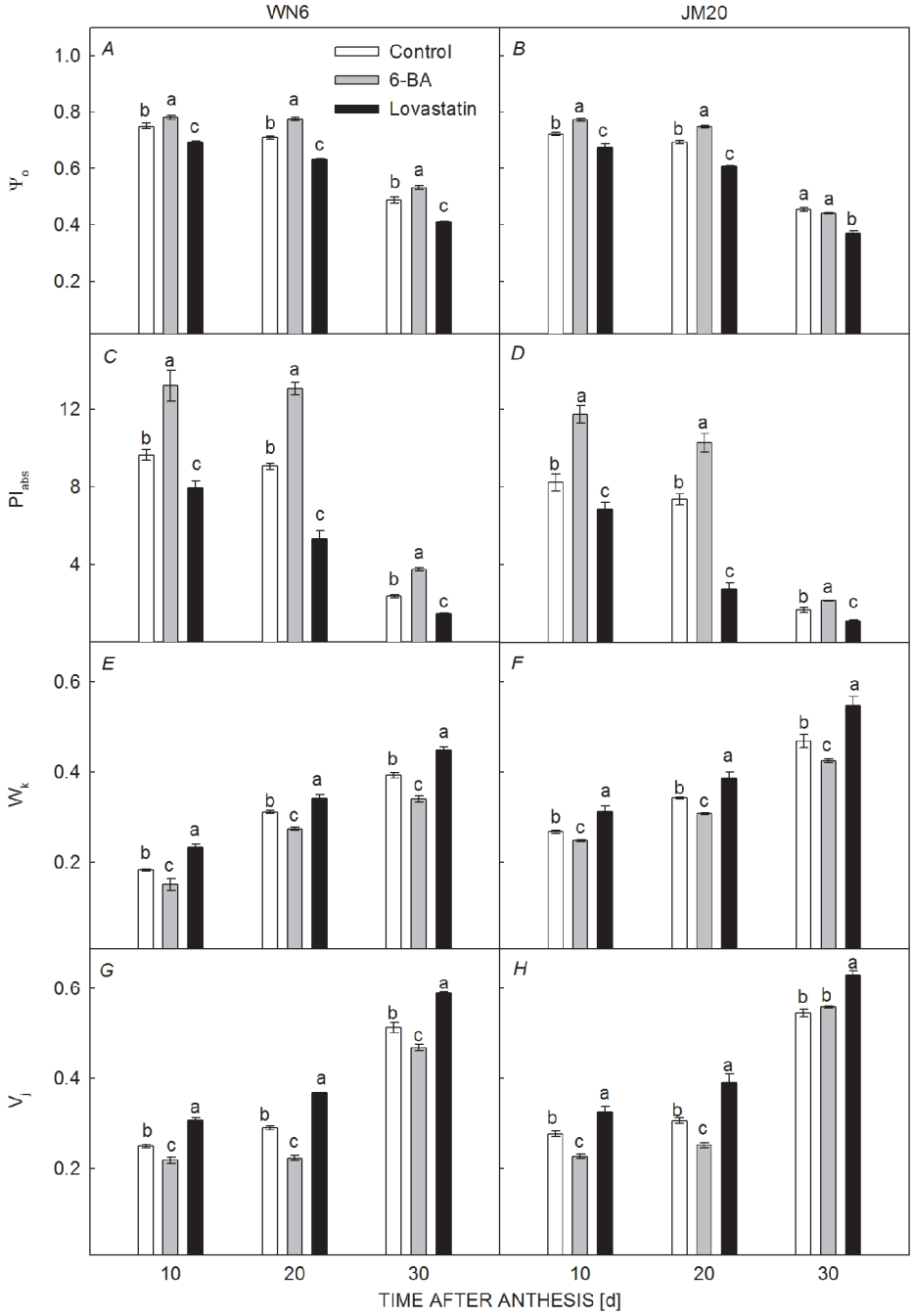

Fig. 6. The effects of 6-BA and lovastatin on probability that a trapped exaction transfers an electron into the electron transport chain beyond QA (Ψo) (*A,B*) and performance index based on absorption of light energy (PIabs) (*C,D*), relative variable fluorescence for the normalization between Fo and Fk (Wk) (*E,F*) and relative variable fluorescence intensity at the J-step (Vj) (*G,H*) of a stay-green (WN6) and a non-stay-green (JM20) wheat cultivar. The normalized relative variable fluorescence at the K step. The relative variable fluorescence at the J step. The means ± SE of ten replicates are presented. *Different letters* indicate significant differences between treatments at $P<0.05$.

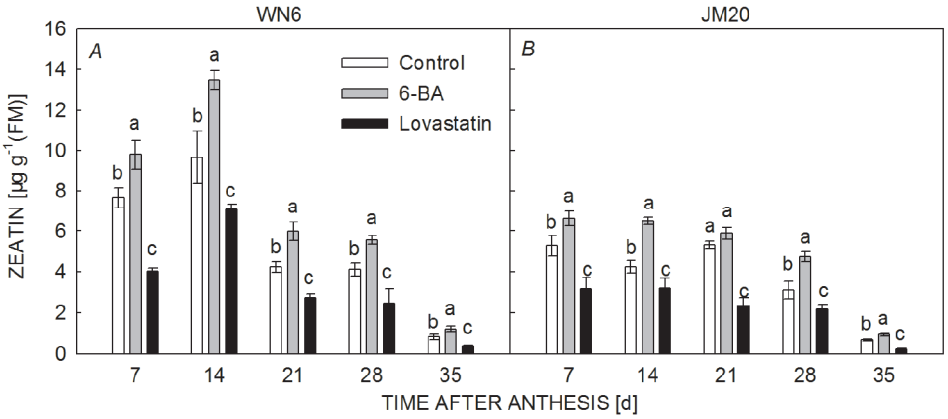

Fig. 7. Effect of 6-BA and lovastatin on zeatin content (Zt) in leaves of a stay-green (WN6) and a non-stay-green (JM20) wheat cultivar. *Vertical bars* represent ± SE of the mean (n = 3). *Different letters* indicate significant differences between treatments at P<0.05.

Chl fluorescence parameters of flag leaves: The maximum quantum yield of the PSII (F_v/F_m), electron transport rate (ETR), and the actual photochemical efficiency (Φ_{PSII}) gradually decreased from 21 to 35 DAA (Fig. 4*E–J*). From 7 to 35 DAA, F_v/F_m, ETR, and Φ_{PSII} of WN6 were greater than those of JM20. Compared with controls, application of 6-BA significantly increased F_v/F_m, ETR, and Φ_{PSII} from 7 to 35 DAA. After the lovastatin treatment, F_v/F_m, ETR, and Φ_{PSII} were all significantly decreased.

Changes in the Chl *a* fluorescence transients: The J-step (2 ms) in the Chl fluorescence transients of JM20 obviously increased by the lovastatin treatment (Fig. 5). Using WN6 treated with 6-BA as a reference (Fig. 5*B*), results showed that the peaks of ΔV_t curves of JM20 appeared at the J-step under the lovastatin treatment, whereas the peaks of WN6 appeared around at the I-step. The amplitudes of the J- and I-step in the control treatment of JM20 were greatly higher than these of WN6. The amplitudes of the J- and I-steps of JM20 greatly decreased by 6-BA, but increased by the lovastatin treatment.

Changes in PSII performance: Probability of transferring electrons to other electron acceptors downstream of Q_A in the electron transport chain (Ψ_o) and the performance indicator (PI_{abs}) were shown in Fig. 6*A,B*. Compared with the control treatment, both Ψ_o and PI_{abs} in the two cultivars significantly increased by exogenous 6-BA application. Ψ_o and PI_{abs} in WN6 significantly increased by 9.4 and 44.2% at 20 DAA, respectively, compared with the controls. Similarly, these parameters increased in JM20 by 7.8 and 39.3%, respectively. In contrast, application of lovastatin significantly decreased Ψ_o and PI_{abs}.

Changes in PSII donors/acceptors: The normalized relative variable fluorescence at the K-step (W_k) and relative variable fluorescence at the J-step (V_j) were presented in Fig. 6*C,D*. W_k and V_j of 6-BA-treated plants significantly decreased. These parameters decreased in JM20 by 7.3 and 17.7%, respectively. However, W_k and V_j of the lovastatin-treated plants obviously increased. These observations indicated that the electron transfer capability of both the donor and the acceptor sides of PSII reaction center was improved by cytokinin.

Content of zeatin (Zt) in flag leaves: The Zt content in both cultivars was high from 7 to 14 DAA, but decreased sharply from 21 to 35 DAA (Fig. 7). Zt contents of SG wheat WN6 were greater than those of JM20 from 7 to 14 DAA. Compared with the control treatment, 6-BA application significantly increased the Zt content in leaves of both cultivars. However, spraying lovastatin markedly decreased the Zt content of WN6 and JM20 from 7 to 35 DAA.

Relationships of Zt content in leaves to antioxidant enzyme activities, Chl and MDA contents, and photosynthetic parameters: Correlation analysis indicated that the Zt content in flag leaves was significantly and positively correlated with Chl contents (Fig. 8*A*), whereas significantly and negatively correlated with MDA contents (Fig. 8*B*). The Zt content was significantly positively correlated with the SOD (r = 0.83**, p<0.01), POD (r = 0.62**, p<0.01), CAT (r = 0.83**, p<0.01), and APX (r = 0.90**, p<0.01) activities (Fig. 8*C–F*). The Zt content in flag leaves was significantly and positively correlated with P_N, F_v/F_m, ETR, and Φ_{PSII} (Fig. 8*G–J*).

Discussion

Stay-green wheat mutant lines maintain longer Chl contents and photosynthetic competence than that of the parental genotype (De Simone *et al.* 2014). In this study, we reported that WN6 showed delayed leaf senescence compared to JM20, on account of the endogenous Zt content, antioxidant capacity, and photosynthetic parameters of flag leaves during the period from flowering to senescence. The leaves of WN6 had the higher Zt content

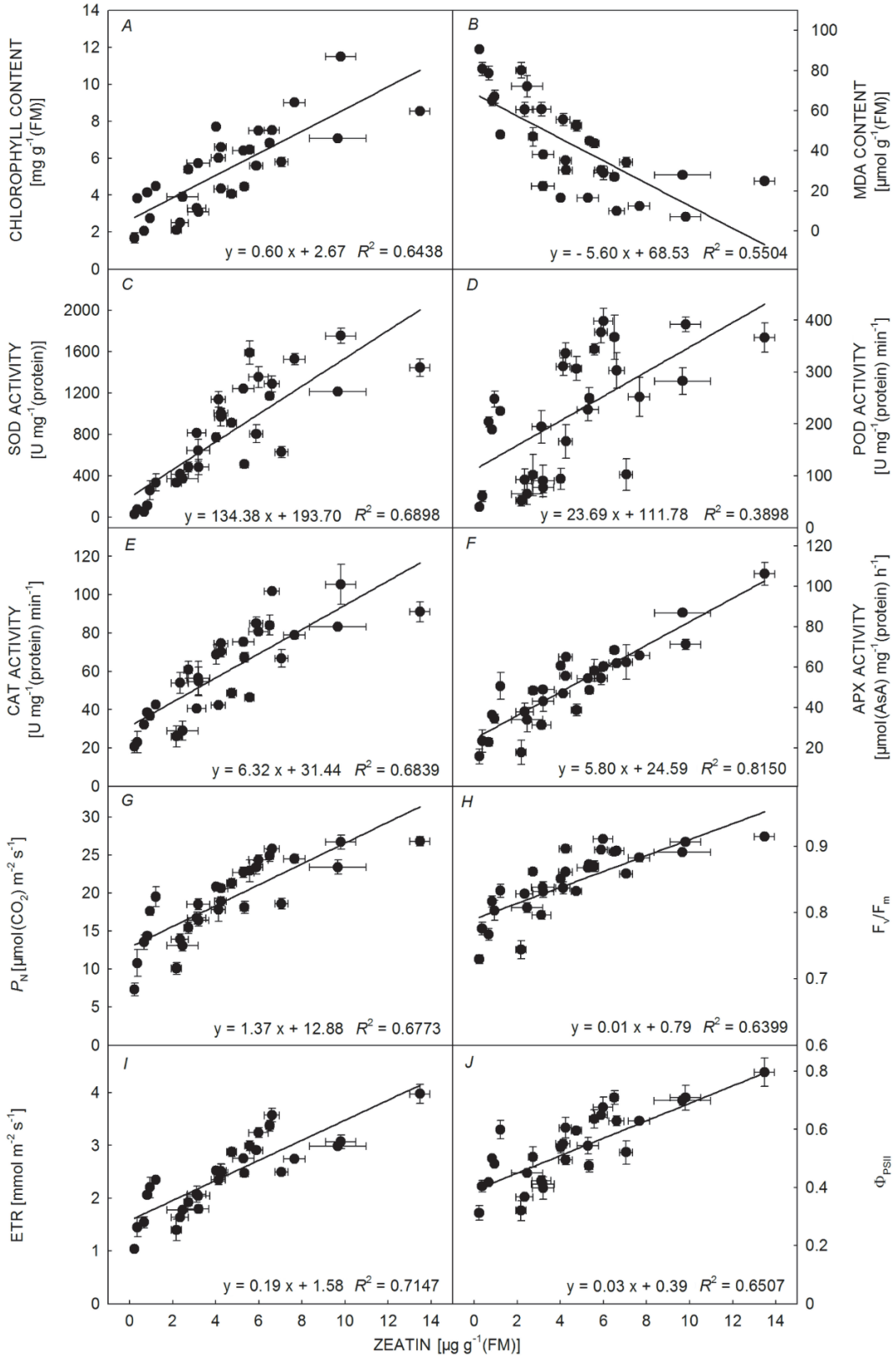

Fig. 8. The relationship between zeatin (Zt) content and chlorophyll, malondialdehyde (MDA) content, superoxide dismutase (SOD), peroxidase (POD), catalase (CAT), ascorbate peroxidase (APX) activity, net photosynthetic rate (P_N), maximal quantum yield of PSII photochemistry (F_v/F_m), electron transport rate (ETR), and effective quantum yield of PSII photochemistry (Φ_{PSII}).

than that of JM20. Kusaba *et al*. (2013) stated that stay-green mutants regulate leaf senescence through a complex signaling network, including cytokinin signaling. Moreover, it has been indicated that Zt could induce expression of response regulator genes, which play major roles in controlling cytokinin-mediated leaf senescence (Hwang and Sheen 2001, Kim *et al*. 2006). WN6 exhibited much higher antioxidant enzyme activities. And therefore, WN6 exhibited the lesser lipid peroxidation, marked with the lower MDA content during leaf senescence. WN6 had the higher Chl content and P_N, compared with JM20. The P_N in WN6 was in agreement with its higher F_v/F_m, ETR, and Φ_{PSII}. In addition, the JIP-test showed that W_k and V_j in stay-green WN6 was lower than that in JM20. Ψ_o and PI_{abs} in WN6 was higher than that in JM20. These results suggest that the oxygen-evolving complex of WN6 was less damaged during leaf senescence. The electron transfer capability of both the donor and the acceptor sides at the PSII reaction center of WN6 was greater than that of JM20. Therefore, WN6 showed higher photosynthetic capacity resulting in an increase in translocation of photo-assimilates to grains. Finally, WN6 had a much higher grain mass.

Cytokinins play important roles in regulating leaf senescence and protecting photosynthetic machinery (Gan *et al*. 1995, Chernyad'ev 2009). Application of cytokinin resulted in increased photochemical quenching and protected the PSII against overexcitation (Ogweno *et al*. 2010). Exogenous cytokinin application maintained higher antioxidant contents and lesser lipid peroxidation (Liu and Huang 2002). In this experiment, the external application of 6-BA significantly increased Chl content and reduced MDA content. This can be explained by the improvement of antioxidant capacity. SOD, POD, CAT, and APX activities in leaves of WN6, especially JM20, were significantly improved by application of 6-BA. In the present study, application of 6-BA resulted in increases in the endogenous Zt content. Whereas, lovastatin reduced the Zt content. Correlation analysis showed that endogenous Zt content was significantly and positively correlated with each antioxidant enzyme activity, and negatively correlated with MDA content. The results suggested that exogenous 6-BA improved the antioxidant enzymes activities of flag leaves and reduced membrane lipid peroxidation owing to increases in endogenous Zt. There are also studies indicating that enhanced endogenous cytokinin content in tobacco plants could prevent the degradation of photosynthetic protein complexes (Rivero *et al*. 2010). Results showed that F_v/F_m in the bentgrass was significantly increased by zeatin riboside (Wang *et al*. 2013). In this study, the P_N of the two wheat cultivars was improved by application of 6-BA; however, lovastain treatment decreased photosynthesis. Analysis of Chl flurescence induction curves allows the evaluation of the physiological condition of photosystem and photosynthetic electron transport chain components (Kalaji *et al*. 2016). The results of the present study revealed that the relative fluorescence kinetics showed that the most distinct peaks in the ΔV_t appeared at J- and I-step (Fig. 5). Exogenous 6-BA enhanced F_v/F_m, ETR, and Φ_{PSII}. Further, 6-BA increased Ψ_o and PI_{abs}, and decreased W_k and V_j in the two cultivars (Fig. 6). This indicated that spraying 6-BA reduced the damage of oxygen-evolving complex and improved the electron transfer capability of both the donor and the acceptor sides at PSII reaction center. Contrary, application of lovastatin had the opposite effects, suggesting that decrease in Zt content could promote PSII reaction centers inactivation, and further validated the protective effect of exogenous 6-BA on PSII.

Based on our results and those reported in previous studies, we can summarize that the increase of grain mass under exogenous 6-BA treatment was closely associated with the changed content of Zt in flag leaves that resulted in higher antioxidant enzyme activities, exerted an important role in reduction of MDA. On the other hand, the increased photosynthetic rate could partially result from the improved PSII performance which facilitated more photosynthate formation.

References

Apel K., Hirt H.: Reactive oxygen species: metabolism, oxidative stress, and signal transduction. – Annu. Rev. Plant Biol. **55**: 373-399, 2004.

Baker N.R., Rosenqvist E.: Applications of chlorophyll fluorescence can improve crop production strategies: an examination of future possibilities. – J. Exp. Bot. **55**: 1607-1621, 2004.

Chernyad'ev I.I.: The protective action of cytokinins on the photosynthetic machinery and productivity of plants under stress (review). – Appl. Biochem. Micro+ **45**: 351-362, 2009.

Crowell D.N., Salaz M. S.: Inhibition of growth of cultured tobacco cells at low concentrations of lovastatin is reversed by cytokinin. – Plant Physiol. **100**: 2090-2095, 1992.

De Simone V., Soccio M., Borrelli G.M. *et al*.: Stay-green trait-antioxidant status interrelationship in durum wheat (*Triticum durum*) flag leaf during post-flowering. – J. Plant Res. **127**: 159-171, 2014.

Gan S., Amasino R.M.: Inhibition of leaf senescence by auto-regulated production of cytokinin. – Science **270**: 1986-1988, 1995.

Hörtensteiner S.: Stay-green regulates chlorophyll and chlorophyll-binding protein degradation during senescence. – Trends Plant Sci. **14**: 155-162, 2009.

Hu L., Wang Z., Huang B.: Growth and physiological recovery of kentucky bluegrass from drought stress as affected by a synthetic cytokinin 6-benzylaminopurine. – Crop Sci. **52**: 2332-2340, 2012.

Hwang I., Sheen J.: Two-component circuitry in *Arabidopsis* cytokinin signal transduction. – Nature **413**: 383-389, 2001.

Kalaji H.M., Jajoo A., Oukarroum A. *et al*.: Chlorophyll *a* fluorescence as a tool to monitor physiological status of plants under abiotic stress conditions. – Acta. Physiol. Plant. **38**: 102-113, 2016.

Khanna-Chopra R.: Leaf senescence and abiotic stresses share reactive oxygen species-mediated chloroplast degradation. – Protoplasma **249**: 469-481, 2012.

Kim H.J., Ryu H., Hong S.H. *et al*.: Cytokinin-mediated control of leaf longevity by AHK3 through phosphorylation of ARR2 in *Arabidopsis*. – P. Natl. Acad. Sci. USA **103**: 814-819, 2006.

Klerk G.J.D., Hanecakova J., Jasik J.: The role of cytokinins in rooting of stem slices cut from apple microcuttings. – Plant Biosyst. **135**: 79-84, 2001.

Kobayashi K., Suzuki M., Tang J. *et al*.: Lovastatin insensitive 1, a novel pentatricopeptide repeat protein, is a potential regulatory factor of isoprenoid biosynthesis in *Arabidopsis*. – Plant Cell Physiol. **48**: 322-331, 2007.

Kusaba M., Tanaka A., Tanaka R.: Stay-green plants: what do they tell us about the molecular mechanism of leaf senescence. – Photosynth Res. **117**: 221-234, 2013.

Lim P.O., Kim H.J., Nam H.G.: Leaf senescence. – Annu. Rev. Plant Biol. **58**: 83-111, 2007.

Liu X.Z., Huang B. R.: Cytokinin effects on creeping bentgrass response to heat stress. II: leaf senescence and antioxidant metabolism. – Crop Sci. 42: 466-72, 2002.

Long S.P., Zhu X.G., Naidu S.L. *et al*.: Can improvement in photosynthesis increase crop yields? – Plant Cell Environ. **29**: 315-330, 2006.

Maxwell K., Johnson G.N.: Chlorophyll fluorescence - a practical guide. – J. Exp. Bot. **51**: 659-668, 2000.

Maxwell K.: Resistance is useful: diurnal patterns of photosynthesis in C3 and crassulacean acid metabolism epiphytic bromeliads. – Funct. Plant. Biol. **29**: 679-687, 2002.

Merewitz E.B., Gianfagna T., Huang B.: Protein accumulation in leaves and roots associated with improved drought tolerance in creeping bentgrass expressing an *ipt* gene for cytokinin synthesis. – J. Exp. Bot. **62**: 5311-5333, 2011.

Mittler R.: Oxidative stress, antioxidants and stress tolerance. – Trends Plant Sci. **7**: 405-410, 2002.

Navabpour S., Morris K., Allen R. *et al*.: Expression of senescence enhanced genes in response to oxidative stress. – J. Exp. Bot. **54**: 2285-2292, 2003.

Nishiyama Y., Allakhverdiev S. I., Murata N.: A new paradigm for the action of reactive oxygen species in the photoinhibition of photosystem II. – BBA-Bioenergetics **1757**: 742-749, 2006.

Ogweno O.J., Hu W.H., Song X.H. *et al*.: Photoinhibition-induced reduction in photosynthesis is alleviated by abscisic acid, cytokinin and brassinosteroid in detached tomato leaves. – Plant Growth Regul. **60**: 175-182, 2010.

Pfannschmidt T.: Chloroplast redox signals: how photosynthesis controls its own genes. – Trends Plant Sci. 8: 33-41, 2003.

Pospíšil P.: Molecular mechanisms of production and scavenging of reactive oxygen species by photosystem II. – BBA-Bioenergetics **1817**: 218-231, 2012.

Pružinská A., Tanner G., Aubry S. *et al*.: Chlorophyll breakdown in senescent *Arabidopsis* leaves. Characterization of chlorophyll catabolites and of chlorophyll catabolic enzymes involved in the degreening reaction. – Plant Physiol. **139**: 52-63, 2005.

Rajcan I., Tollenaar M.: Source:sink ratio and leaf senescence in maize: I. Dry matter accumulation and partitioning during grain filling. – Field Crop. Res. **60**: 245-253, 1999.

Rivero R.M., Gimeno J., Van Deynze A. *et al*.: Enhanced cytokinin synthesis in tobacco plants expressing PSARK: IPT prevents the degradation of photosynthetic protein complexes during drought. – Plant Cell Physiol. **51**: 1929-1941, 2010.

Schansker G., Srivastava A., Govindjee *et al*.: Characterization of the 820-nm transmission signal paralleling the chlorophyll *a* fluorescence rise (OJIP) in pea leaves. – Funct. Plant Biol. **30**: 785-796, 2003.

Shiferaw B., Smale M., Braun H.J. *et al*.: Crops that feed the world 10. Past successes and future challenges to the role played by wheat in global food security. – Food Secur. **5**: 291-317, 2013

Strasser B.J.: Donor side capacity of Photosystem II probed by chlorophyll a fluorescence transients. – Photosynth. Res. **52**: 147-155, 1997.

Strasser R.J., Srivastava A., Tsimilli-Michael M.: The fluorescence transient as a tool to characterize and screen photosynthetic samples. – In: Yunus M., Pathre U., Mohanty P. (ed.): Probing Photosynthesis: Mechanism, Regulation and Adaptation. Pp. 445-483. Taylor and Francis Press, London 2000.

Thomas H., Howarth C.J.: Five ways to stay green. – J. Exp. Bot. **51**: 329-337, 2000.

Thomas H., Ougham H.: The stay-green trait. – J. Exp. Bot. **65**: 3889-3900, 2014.

Tjus S.E., Scheller H.V., Andersson B. *et al*.: Active oxygen produced during selective excitation of photosystem I is damaging not only to photosystem I, but also to photosystem II. – Plant Physiol. **125**: 2007-2015, 2001.

Wang K.H., Zhang X.Z., Ervin E.: Effects of nitrate and cytokinin on creeping bentgrass under supraoptimal temperatures. – J. Plant Nutr. **36**: 1549-1564, 2013.

Werner T., Motyka V., Strnad M. *et al*.: Regulation of plant growth by cytokinin. – P. Natl. Acad. Sci. USA **98**: 10487-10492, 2001.

Yaronskaya E., Vershilovskaya I., Poers Y. *et al*.: Cytokinin effects on tetrapyrrole biosynthesis and photosynthetic activity in barley seedlings. – Planta **224**: 700-709, 2006.

Zadoks J.C., Chang T.T., Konzak C F.: A decimal code for growth stages of cereals. – Weed Res. **14**: 415-421, 1974.

Zavaleta-Mancera H.A., López-Delgado H., Loza-Tavera H. *et al.*: Cytokinin promotes catalase and ascorbate peroxidase activities and preserves the chloroplast integrity during dark-senescence. – J. Plant Physiol. **164**: 1572-1582, 2007.

Zhao M.R., Han Y.Y., Feng Y.N. *et al*.: Expansins are involved in cell growth mediated by abscisic acid and indole-3-acetic acid under drought stress in wheat. – Plant. Cell. Rep. **31**: 671-685, 2012.

Zhao S.J., Shi G.A., Dong X.C.: [Experimental guide for plant physiology.] – In: Liu X.C., Li G. (ed.): Techniques of Plant Physiological Experiment. Pp. 134-142. China Agric. Sci. Technol. Press, Beijing 2002. [In Chinese]

Zhu X.G., Long S.P., Ort D.R.: Improving photosynthetic efficiency for greater yield. – Annu. Rev Plant Biol. **61**: 235-261, 2010.